*Physics of Complex Systems, 2024, vol. 5, no. 4*
*www.physcomsys.ru*

*Physics of Semiconductors.*
*Physics of thin films*

UDC 538.9
EDN THHPQB
https://www.doi.org/10.33910/2687-153X-2024-5-4-205-214

# The formation of $MoTe_2$ nanofilms on metal substrates

P. N. Yakushev [1], V. A. Bershtein [1], A. V. Kolobov ✉[2]

[1] Ioffe Institute, 26 Polytechnicheskaya Str., Saint Petersburg 194021, Russia
[2] Herzen State Pedagogical University of Russia, 48 Moika Emb., Saint Petersburg 191186, Russia

***Authors***
Pavel N. Yakushev, ORCID: 0000-0002-9947-1245, e-mail: yak@pav.ioffe.ru
Vladimir A. Bershtein, ORCID: 0000-0003-4524-8766, e-mail: vbersht.polmater@mail.ioffe.ru
Alexandr V. Kolobov, ORCID: 0000-0002-8125-1172, e-mail: akolobov@herzen.spb.ru

***For citation:*** Yakushev, P. N., Bershtein, V. A., Kolobov, A. V. (2024) The formation of $MoTe_2$ nanofilms on metal substrates. *Physics of Complex Systems*, 5 (4), 205–214. https://www.doi.org/10.33910/2687-153X-2024-5-4-205-214 EDN THHPQB

***Received*** 22 September 2024; reviewed 28 September 2024; accepted 09 October 2024.

***Funding:*** This work was partially supported by the Russian Science Foundation (grant 22-19-00766).

***Abstract.*** Transition-metal dichalcogenides are among most studied two-dimensional semiconductors for applications in electronics, optoelectronics, spintronics, and memory devices. One of the simple commercially friendly methods to fabricate thin crystalline films is solid-state crystallization from the amorphous phase. In this work, using differential scanning calorimetry (DSC) measurements, we demonstrate that $MoTe_2$ nanolayers deposited on different substrates (Ta, Al, W, Mo) manifest distinctly different crystallization behavior. We argue that these differences are associated with different chemical affinity of the film constituents towards the substrate material and propose a scheme of this complex crystallization process.

***Keywords:*** transition-metal dichalcogenides, solid-state crystallization, differential scanning calorimetry, nanofilms, two-dimensional semiconductors

## Introduction

The success of graphene has triggered an intensive search for other two-dimensional (2D) materials, especially 2D semiconductors. One of the promising classes of such materials is transition-metal dichalcogenides (TMDCs) (Kolobov, Tominaga 2016) with the generic formula $MX_2$ (M = Mo, W, X = S, Se, Te). These materials possess a layered structure, where M-X-M sandwiches, often called monolayers, are held together by weak van der Waals forces. The interest in these materials was reignited about ten years ago when it was found that the electronic structure of $MoS_2$ changed from indirect in the bulk form to a direct gap in the monolayer limit (Mak et al. 2010), which makes TMDCs an important class of optoelectronic materials. Unique properties of 2D TMDCs were reported. Among them are extremely large exciton binding energies (Chernikov et al. 2014), spin-valley coupling (Xiao et al. 2012), etc. Numerous and various devices based on few-layer and monolayer TMDCs have been demonstrated, ranging from various electronics (Cho et al. 2015; Lin et al. 2014; Sarkar et al. 2015), optoelectronics (Yin et al. 2016), and spintronics (Suzuki et al. 2014) applications to biomedical uses (Liu, Liu 2018).

An additional benefit of using monolayer thick semiconductors as active layers in devices is their ultra-low power consumption (Tang et al. 2023). The sub-nanometer thickness of such layers also enables the use of few monolayer TMDC in transparent and flexible electronics (Li et al. 2020). Monolayer-thick 2D materials are usually very strong mechanically, which opens the possibility to further control their electronic structure and properties through the application of strain (straintronics) (Wei et al. 2017).

While most 2D transition-metal dichalcogenides (TMDCs) possess only one single phase stable at room temperature, 2D $MoTe_2$ exhibits intriguing polymorphism: the semi- conducting 2H phase and the metallic 1T' phase. In the semiconducting 2H phase, the Mo and Te atoms are arranged in in-plane hexagonal symmetry and out-of-plane trigonal prismatic coordination with a space group of $P6m2$. In the metallic 1T' phase, they are arranged in in-plane monoclinic symmetry and out-of-plane octahedral coordination with a space group of $P12_1/m1$ (Huang et al. 2016). A remarkable feature of this material is that the energy barrier between the two states is rather low (Duerloo 2014), which enables an easy transition between these states. The transition can be driven thermally or, alternatively, stimulated by supplying external energy by means of strain (Song et al. 2016) or electronic excitation (Cho et al. 2015; Kolobov et al. 2016; Li et al. 2016).

Bulk $MoTe_2$ can be directly synthesized in either a semiconducting 2H or a metallic 1T' phase (Park et al. 2015; Yoo et al. 2017; Zhou et al. 2015), while both phases are stable at temperatures up to 815 °C and 900 °C, respectively (Ueno, Fukushima 2015). The fabrication methods for monolayer thick structures can be classified into two broad categories, namely, top-down methods and bottom-up methods. In the top-down approach, nanolayers are produced by removing building blocks from the bulk phase to generate the desired structure. Bottom-up synthesis, on the other hand, involves the formation of a nanostructure by stacking up atoms, molecules or other nanoparticles. This process generally uses two methods: physical and/or chemical synthesis. In the former, the constituents of the nanolayers are deposited physically during the fabrication process. The most common method is physical vapor deposition where vapour moieties are condensed through processes such as sputtering or evaporation. In chemical synthesis, chemical reactions are involved as in the chemical vapor deposition (CVD) process.

In most of the reported cases, devices were made from monolayer TMDCs manually exfoliated from a bulk crystal. This approach, while important in proof-of-principle studies, is not suitable, however, for industrial applications. The latter need a simple industry-friendly method to fabricate thin TMDC crystals. The lack of a reliable large-area synthesis process greatly hinders their practical use. An alternative is bottom-up fabrication methods such as chemical vapour transport. This method allows one to fabricate thin layers of TMDC and significant progress has been recently made, but the area of the grown samples remains small, which is also insufficient for mass production of devices. In addition, it requires very high temperatures.

When proof-of-principle results have to be transformed to an industrial scale, a user-friendly cheap mass production technology is needed. One such approach is to use sputtering to fabricate amorphous films with subsequent solid-state crystallization. This approach is more suitable than many alternatives from the viewpoint of cost and productivity since sputtering is a well-established fabrication method, which has long been used for thin film production, for example, of semiconductor devices and optical media. Successful uses of this method have been demonstrated for various transition-metal dichalcogenide films (Hatayama et al. 2022; Huang et al. 2017; 2019; Krbal et al. 2021).

The crystallization process of transition-metal dichalcogenides is unique. Generally, amorphous solids possess the local structure similar to that of the parent crystals, which is known as the Zachariasen paradigm (Zachariasen 1932) stating that glasses must be considered as a media maintaining the local bonding structure of their parent crystals and where only the long-range order is missing. In transition-metal dichalcogenides the situation is fundamentally different. An amorphous solid is isotropic (3D), whereas TMDCs in the crystalline form are layered 2D materials. Consequently, the crystallization of TMDC nanofilms involves lattice dimensionality change, i. e., a 3D-2D transition, which makes this process interesting from the basic physics perspective.

For $MoTe_2$ this transformation is even more complex because of its polymorphism. A multi-step process for recrystallizing 2H-$MoTe_2$ was previously reported (Hatayama et al. 2022; Huang et al. 2017). Namely, as-sputtered amorphous $MoTe_2$ film first crystallizes into the 1T'-phase. It was argued to be a consequence of favorable strain condition in the encapsulated structure (Song et al. 2016), the presence of local tellurium vacancies in the amorphous film (Zhou et al. 2016), and/or potential pre-existence of 1T' nucleation sites. Subsequently, at higher temperatures, the 1T'-MoTe film recrystallizes into a homogeneous 2H-$MoTe_2$ phase. At specific heating conditions the film may directly crystallize into the 2H phase.

Another feature of 2D crystallization is the very unusual sequences of changes in the short and long-range order. While typically crystallization can be viewed as the establishment of the long-range order with the pre-existing short-range order (the same in the amorphous and crystalline phases), in the case of 2D crytallization, long range order (the formation of the layered structure) may be established first, with chemical ordering coming into play later (Saito et al. 2021).

Schematically, the process is illustrated in Fig. 1. Figure 1 (right panel) shows the effect of the annealing temperature and time on the obtained polymorphic structure. According to the shown phase diagram, for annealing temperatures of 500 °C and below the $MoTe_2$ film remained in the amorphous phase for annealing times as long as 30 hours (Huang et al. 2019). In contrast, in (Hatayama et al. 2022) crystallization of the amorphous $MoTe_2$ film was reported to start at temperatures just above 300 °C. The observed differences may be explained by different thicknesses of the films in the two cases and/or existing strains. The presence of strain is known to have a significant effect on the structural relaxation processes in chalcogenide films (Kolobov et al. 1982; Raoux et al. 2008; Simpson et al. 2010).

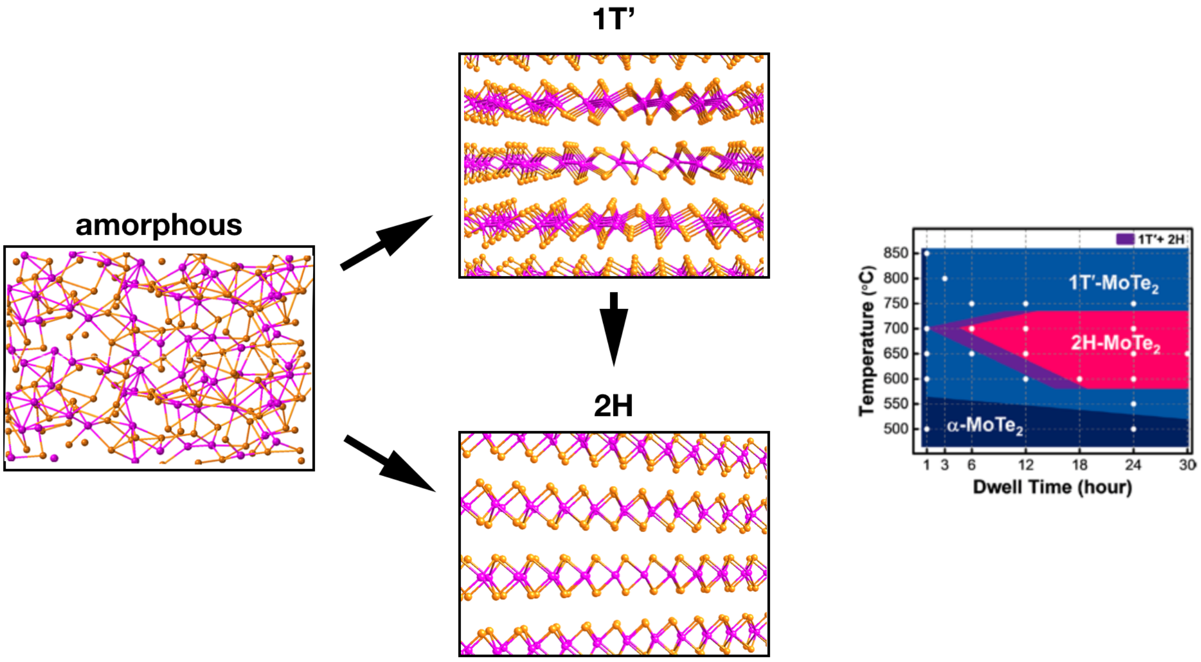

Fig. 1. Schematics of the amorphous $MoTe_2$ crystallization process: depending on the treatment conditions an amorphous film may initially crystallize to the 1T’ phase and then to the 2H phase or directly to the 2H phase. The right panel shows the phase diagram after ref. (Huang et al. 2019)

It should be noted that crystallization of TMDC requires heating to relatively low temperatures compared to the process of direct synthesis of the crystalline phase. Indeed, chemical vapor transportation, which is a common method for synthesizing both 2H- and 1T’-$MoTe_2$ bulk materials through a chemical reaction between mixed Mo and Te powders, requires exposure to temperatures on the order of 1100 °C for tens of hours.

At the same time, this solid-state crystallization temperature is sufficiently high to ensure potential chemical interaction of the amorphous film with a substrate. This process, obviously, depends on the substrate material and its chemical reactivity with the components of the film. A solid-state reaction between the substrate and an amorphous TMDC film is especially likely when the substrate is metallic and such situations may exist during devices fabrication process when a film has to be deposited on a metallic contact. The likelihood of such an interaction increases further when the metal belongs to the class of transition metals that can form transition-metal dichalcogenides.

The strong effect of the substrate materials on the formation of oriented 2D crystalline layers was observed by some of the present authors when amorphous $Sb_2Te_3$ films were grown by magnetron sputtering (Saito et al. 2015). In the cited work, a novel deposition mechanism based on the selective reactivity of the constituent elements of the film (Sb, Te) and the substrate materials giving rise to van der Waals epitaxy was proposed based on the analysis of the binary phase diagrams of (a) Sb–W, (b) Te–W, (c) Sb–Si, (d) Te–Si, (e) Sb–O, and (f) Te–O systems (Bailey 1966; Boller, Nowotny 1964; Knop, Haraldsen 1956; Thurmond, Kowalchik 1960) (see ref. (Saito et al. 2015)). These diagrams could be divided into three classes: one class having no compounds or solid solutions, while for other combinations compounds are formed. In the latter case, compounds with either just one constituent element selectively or with both of them may be formed. In cases when no compounds are formed or both Sb and Te species can chemically react with the substrate materials, amorphous or polycrystalline films were formed. On the other hand, the use of substrates where Sb did not form a compound with the substrate, while Te did, resulted in significantly different sticking coefficients for the two kinds of atoms, i. e., when Sb and Te atomic species from the plasma reached the substrate, the surface was initially covered with a quasi-monolayer of Te thus passivating the surface.

Upon subsequent film growth the layers became oriented with respect to the substrate. This growth method, called self-organized epitaxy of layered materials was demonstrated to be an efficient industry-friendly fabrication method. It can be speculated that when an amorphous film deposited on a substrate is heated, the selectivity of the substrate material to its constituent elements will also significantly affect the crystallization process. In particular, the film may crystallize (i) as a self-standing film simply supported by the substrate, or (ii) the substrate materials may also be involved in the crystallization process. Furthermore, tellurium is known to crystallize at temperatures as low as room temperature (Zhao et al. 2021). While the presence of transition metal atoms and Te-metal bonds hinders this process, in an amorphous phase Te-rich regions may exist that may be prone to crystallization.

Consequently, investigation of the crystallization process of TMDC nanofilms is important from both fundamental and applied perspectives. In this work, we have experimentally studied the crystallization process of $MoTe_2$ nanolayers on different metallic substrates using differential scanning calorimetry (DSC).

## Experimental details

Samples were fabricated by magnetron sputtering and were 100 nm thick $MoTe_2$ films deposited on both sides of 20–25 $\mu$m thick foils of four different metals: Al, Ta, Mo, and W. 50 nm nanolayers of $SiO_2$ were additionally sputtered on top of the $MoTe_2$ to prevent oxidation. We note here that three of the metals used (Mo, W, and Ta) form TMDCs while one of them (Mo) is the same as the transition metal in the studied film. Consequently, when amorphous films are prepared by sputtering, chalcogen species arriving at the substrate may interact not only with metal ions deposited from the plasma but also with the substrate, which can have a certain effect on the composition and structure of the grown films as well as on the details of the crystallization process.

DSC measurements were performed using a DSC 6300 calorimeter (Seiko Instruments, Japan) with the heating rate of 10 deg/min in $N_2$ atmosphere; the rate of nitrogen flow was 40 ml/min. The cooling rate after scanning was 20 deg/min. Calibration of the temperature scale and enthalpy effects was performed using indium ($T_m$ = 156.6 °C, $\Delta H_m$ = 28.6 J/g) and zinc ($T_m$ = 419.6 °C, $\Delta H_m$ = 107.5 J/g) standards.

Each studied sample was a stack of 5 mm diameter circles cut from the foil covered on both sides by $MoTe_2$ nanolayers. Depending on the substrate material, the total sample weight varied from 250 to 500 mg, whereas the $MoTe_2$ mass equaled 1–2 mg (see Table 1). This stack was placed into a DSC capsule (aluminium or ceramic) with the internal diameter of 6 mm. The reference was a similar capsule with a stack of the same number of metallic circles cut from the same foil but without $MoTe_2$ and $SiO_2$ nanolayers. The accuracy of the determination of the glass transition temperatures, $T_g$'s, and crystallization temperatures, $T_{cr}$'s, was 1–2 °C, whereas the crystallization enthalpies, $\Delta H_{cr}$'s, could be determined with the accuracy of 20% only due to the limited accuracy of mass determination of $MoTe_2$ samples. DSC curves were obtained in temperature ranges from 200 °C to 900 °C in the cases of Ta, W, and Mo substrates (and ceramic pans), and in a range of 200 °C to 600 °C in the case of Al substrate (and Al pan).

Table 1. DSC characteristics of $MoTe_2$ nanolayers on different substrates

| Substrate | $MoTe_2$ mass,mg | $T_g$, °C | Crystallization range, °C | $T_{cr}^{max}$, °C | Crystallization enthalpy $\Delta H_{cr}$, kj/g |
|---|---|---|---|---|---|
| Ta | 1.8 | 333 | 355–470 | 400 | 18.6 |
| – | – | – | 428–490 | 470 | 3.8 |
| – | – | – | 624–807 | 680 | 3.7 |
| W | 1.6 | 450 | 468–800 | 494 | 3.8 |
| – | – | – | – | 680 | – |
| Al | 1.2 | 468 | 475–560 | 495 | 0.5 |
| Mo | 1.8 | – | – | – | – |

## Results and Discussion

Figure 2 shows the DSC curves for $MoTe_2$ nanolayers on different substrates (foils) obtained in temperature ranges from 200 °C to 600–900 °C. The crystallization ranges, Tg and $T_{cr}^{max}$ values and the crystallization enthalpies $\Delta H_{cr}$ obtained from the measurements are summarized in Table 1.

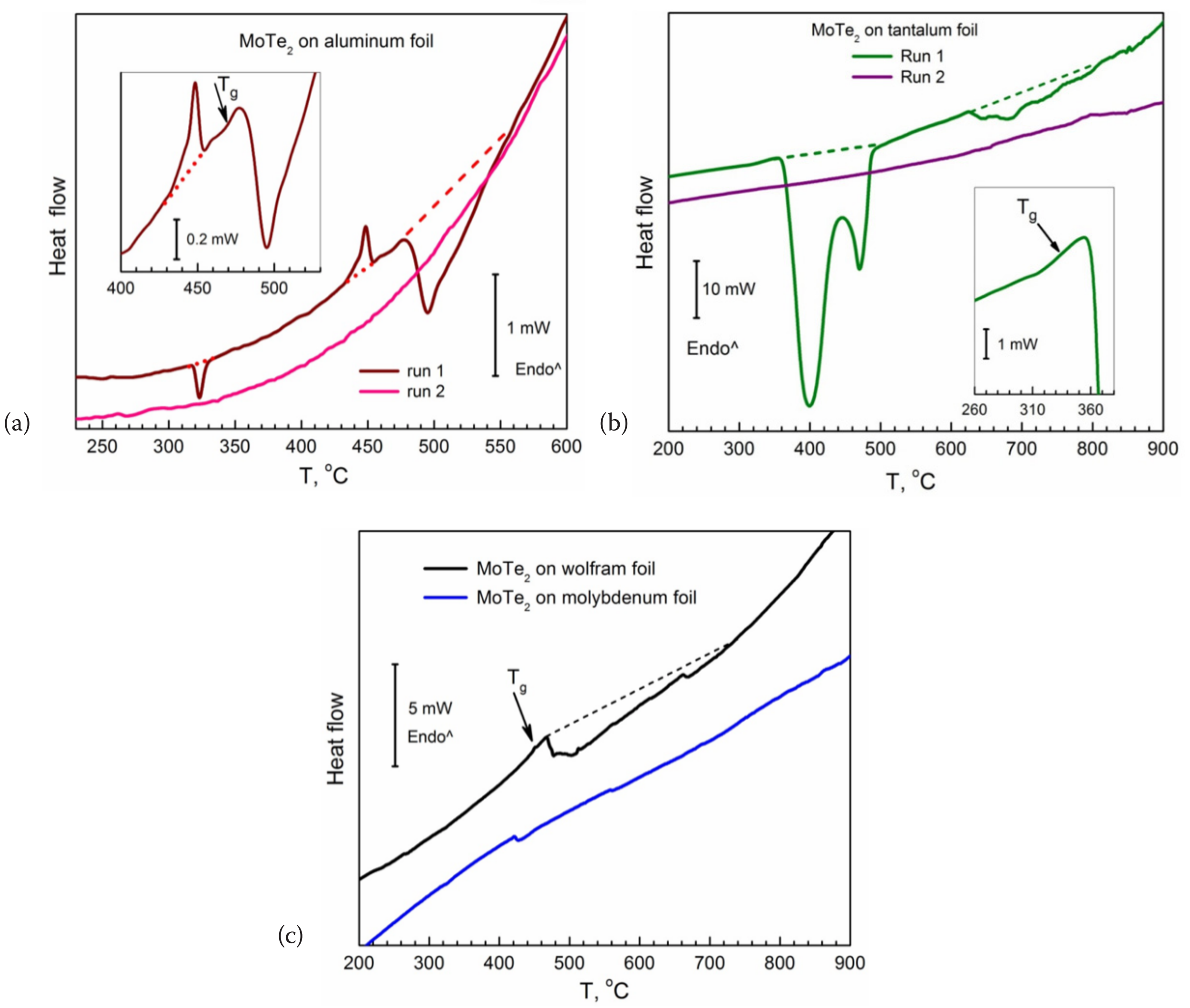

Fig. 2. DSC curves of $MoTe_2$ nanolayers (100 nm thick) during the first and second scans on aluminum (a), tantalum (b) and during the first scan on tungsten and molybdenum foils (c)

One obvious result of these measurements is a drastically different thermal behavior of $MoTe_2$ nanolayers caused by the strong influence of the substrate material on the structural state of deposited nanolayers. Figure 2a shows a DSC curve obtained during the first scan for $MoTe_2$ nanolayers on Al substrate. Several peaks can be clearly observed. The lowest (exothermic) peak at 323 °C can be attributed to the crystallization of Te in the film. The result is consistent with the findings of (Fukuda et al. 2022; Hatayama et al. 2022), where segregation and crystallization of Te upon heating or photoexcitation of an amorphous $MoTe_2$ film to approximately 300 °C was reported. The higher temperature endothermic peak of 445 °C is due to Te melting, which, again, is consistent with the results reported in (Hatayama et al. 2022) and with the literature data (the melting point of pure Te ~ 450 °C).

The relatively high glass-transition temperature around 468 °C (compared with $T_g$ = 350 °C for the film on a tantalum substrate, Fig, 2b) suggests that a film is relatively ordered. Maximal crystallization of the film takes place at 495 °C. A low crystallization enthalpy $\Delta H_{cr}$ in this case further indicates a mixed amorphous-crystalline state of $MoTe_2$ nanolayers, with a high degree of ordering already in the initial nanolayer. The heat capacity step at $T_g$ = 468 °C is also dozens of times smaller than that for $MoTe_2$ nanolayers deposited on a Ta substrate. Therefore, the ‘residual’ crystallization of $MoTe_2$ nanolayers on Al foil occurs at much higher temperatures, starting at 475 °C. According to the literature, this process corresponds to the formation of the 1T' crystalline phase. Regrettably, the use of Al substrate naturally precluded us from continuing the experiment to higher temperatures.

In the case of a Ta substrate, the DSC curve (green) obtained at the first scan and shown in Fig. 2b had a significantly lower glass-transition temperature (333 °C) indicating that the film was in a more disordered phase, as also evidenced by the maximal heat capacity step in this transition, and high crystallization enthalpy $\Delta H_{cr}$. In this case, three regions of the crystallization process at temperatures from 355 °C to 807 °C were observed (Fig. 2b, Table 1). Crystallization starts at a much lower temperature than in the case of an Al substrate and the exothermic peak, corresponding to this process, splits into two peaks. It may be possible that the lower peak is associated with the crystallization of Te, while the crystallization of the $MoTe_2$ phase is associated with the second peak. Finally, a second exothermic (crystallization) peak is observed at temperatures higher than 680 °C. We believe that this transition is associated with the 1T' to 2H transformation, which agrees well with the observations and conclusions made in (Hatayama et al. 2022). The features observed for the films on Al and Ta substrates disappeared in the DSC curves during the second scan after heating up and cooling the sample, clearly demonstrating that they are associated with an irreversible crystallization process.

A rather close initial state of partially ordered $MoTe_2$ nanolayers on W foil was observed although their residual crystallization occurred at heating up to 728 °C (Table 1) and the enthalpies associated with the process are significantly lower. Finally, the DSC curve for $MoTe_2$ nanolayers on Mo substrate did not show any essential features upon heating; there was no exothermic or endothermal effects in the DSC curve even during the first scanning process, which suggests they were to a large extent crystalline already in the as-deposited state (Fig. 2c).

The configuration–energy diagram of the crystallization process of amorphous $MoTe_2$ nanofilms, as revealed by the present results, and its schematic representations are shown in Fig. 3 and Fig. 4, respectively.

Thus, we revealed a drastic influence of the substrate material on the structural state of deposited $MoTe_2$ nanolayers, which demonstrates that the crystallization of amorphous $MoTe_2$ is a very complex process. We propose that the underlying cause is the competition of several processes, viz., (i) the film growth from the particles arriving at the substrate from the target, (ii) thermal behavior of various components of the film, and (iii) the interaction of chalcogen atoms with transition metal ions of the substrate leading to oriented growth of the layered crystal as illustrated schematically in Fig. 5. We note that there is a strong similarity between this process and the process of self-organized van der Waals epitaxial growth of $Sb_2Te_3$ films reported by some of the present authors earlier (Saito et al. 2015).

Based on these results, we can speculate that for oriented growth of layered $MoTe_2$, the substrate material should satisfy one of the following conditions:

- The substrate should have a Te-terminated surface of a properly oriented tellurium compound, such as CdTe.
- The substrate should be made of a material that readily and selectively reacts with Te forming a Te passivation layer, which is the initial step for the oriented growth.
- An advantageous property of a potential substrate is also its flatness. In this case, subsequent growth of the film will proceed in the van der Waals epitaxy mode resulting in the formation of a crystalline film.

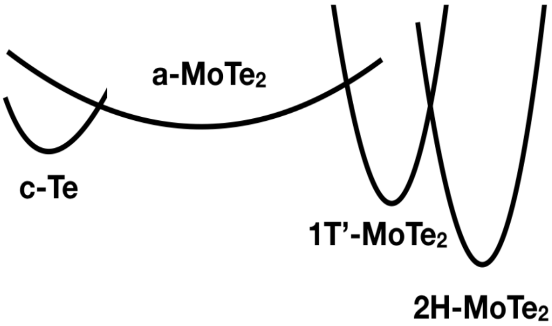

Fig. 3. Configuration–energy diagram describing the $MoTe_2$ crystallization process

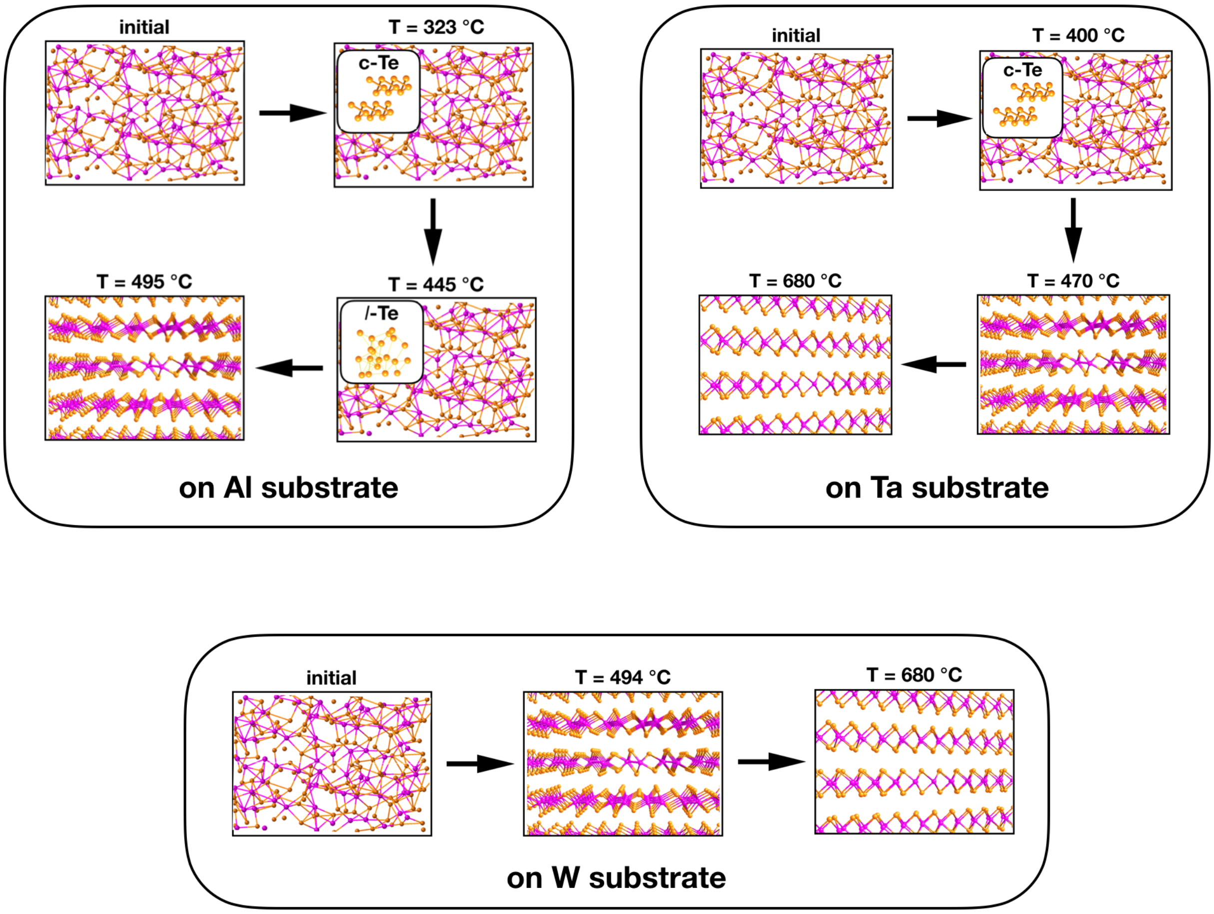

Fig. 4. Schematics of structural evolution of a $MoTe_2$ film deposited on Al, Ta, and W substrates

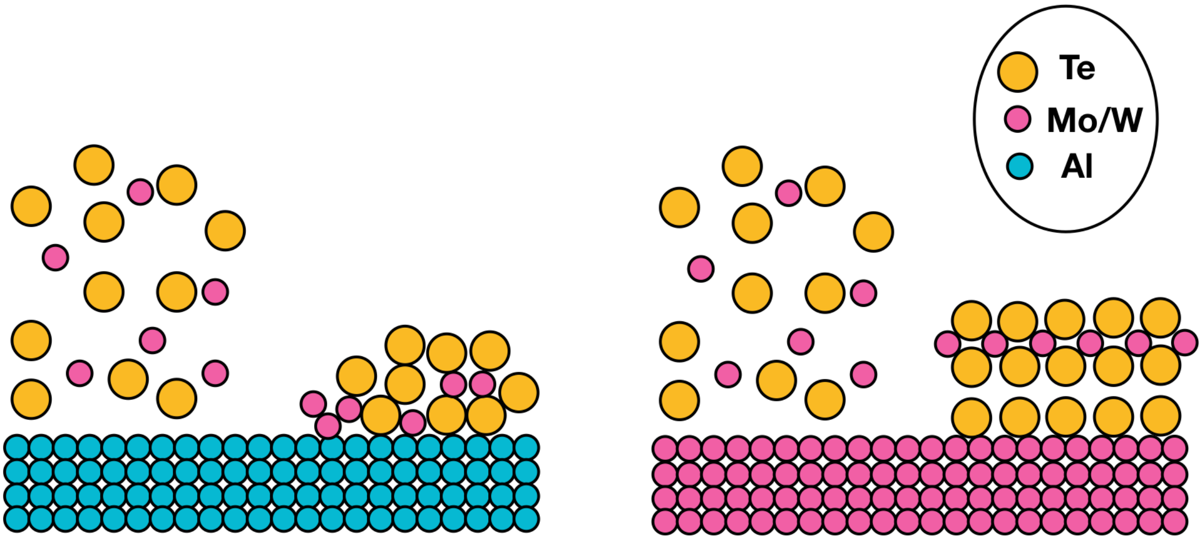

Fig. 5. Schematics of the film growth on an 'inert' substrate such as aluminum/tantalum (left) and on a chemically 'active' substrate such as molybdenum/tungsten (right). In the former case, an amorphous film is formed, while in the latter, strong chemical affinity of the chalcogen atoms in the plasma and TMDC atoms of the substrate results in the growth of a layered crystalline film

Probably the best substrates for this purpose would be terminated surfaces of van der Waals chalcogenides, such as InTe or GaTe of topological insulators such as $Sb_2Te_3$. While most experimental work concentrates on InSe and GaSe, layered tellurides with the similar structure are also stable as was demonstrated based on the absence of imaginary modes in corresponding phonon dispersion spectra (Demirci et al. 2017) The latter are also a 2D semiconductor with covalently bonded blocks having the Te-In-In-Te stacking sequence. While the lattice constants of InTe (4.40 Å) and GaTe (4.13 Å) (Demirci et al. 2017) are both larger than that of $MoTe_2$ (3.55 Å), van der Waals epitaxy has an advantage that it does not depend on the lattice constant difference between the substrate materials and an overlayer. Hypothetically, the chemical nature of the terminated chalcogen species is not important for van der Waals epitaxy, i. e., $MoTe_2$ should grow as a layered material also on a flat Se-terminated surface. In this case, GaSe (with the lattice constant of 3.82 Å) can be a suitable material.

## Conclusions

In conclusion, the fine details of the solid-state crystallization process of amorphous $MoTe_2$ films are known to depend on many aspects such as the film thickness and the heating conditions. Our present results additionally demonstrate a very strong substrate dependence. All these parameters must be taken into consideration when developing technology of $MoTe_2$ film fabrication. We believe that the results obtained for $MoTe_2$ are of general nature and are also applicable to other transition-metal dichalcogenides such as $MoS(e)_2$, $WS(e)_2$ etc. and, possibly, to other classes of van der Waals chalcogenides.

Based on the obtained results we propose a model of the $MoTe_2$ crystallization process and we note that the interpretation of the process based on the DSC studies is very similar to that suggested from direct structural measurements using x-ray diffraction, Raman scattering, and EXAFS (Saito et al. 2015).

## Conflict of Interest

The authors of this work declare that they have no conflicts of interest, either existing or potential.

## Author Contributions

Conceptualization — Alexandr V. Kolobov, Vladimir A. Bershtein; methodology — Vladimir A. Bershtein; investigation — Pavel N. Yakushev; writing (original draft preparation) — Vladimir A. Bershtein; writing (review and editing) — Alexandr V. Kolobov, Vladimir A. Bershtein. All the authors have read and agreed to the published version of the manuscript.

## References

Bailey, L. G. (1966) Preparation and properties of silicon telluride. *Journal of Physics and Chemistry of Solids*, 27 (10), 1593–1598. https://doi.org/10.1016/0022-3697(66)90237-X (In English)

Boller, H., Nowotny, H. (1964) Kristallchemische Untersuchungen in Systemen (Ti, Nb, Ta, Mo, W)–(As, Sb). *Monatshefte für Chemie und Verwandte Teile Anderer Wissenschaften*, 95, 1272–1282. https://doi.org/10.1007/BF00904725 (In English)

Chernikov, A., Berkelbach, T. C., Hill, H. M. et al. (2014) Exciton binding energy and nonhydrogenic Rydberg series in monolayer $WS_2$. *Physical Review Letters*, 113, article 076802. https://doi.org/10.1103/PhysRevLett.113.076802 (In English)

Cho, S., Kim, S., Kim, J. H. et al. (2015) Phase patterning for ohmic homojunction contact in $MoTe_2$. *Science*, 349 (6248), 625–628. https://doi.org/10.1126/science.aab3175 (In English)

Demirci, S., Avazlı, N., Durgun, E., Cahangirov, S. (2017) Structural and electronic properties of monolayer group III monochalcogenides. *Physical Review B*, 95, article 115409. https://doi.org/10.1103/PhysRevB.95.115409 (In English)

Duerloo, K.-A. N., Li, Y., Reed, E. J. (2014) Structural phase transitions in two-dimensional Mo- and W-dichalcogenide monolayers. *Nature Communications*, 5, article 4214. https://doi.org/10.1038/ncomms5214 (In English)

Fukuda, T., Kaburauchi, R., Saito, Y. et al. (2022) Photo-induced tellurium segregation in $MoTe_2$. *physica status solidi (RRL) — Rapid Research Letters*, 16 (9), article 2100633. https://doi.org/10.1002/pssr.202100633 (In English)

Hatayama, S., Saito, Y., Makino, K. et al. (2022) Phase control of sputter-grown large-area $MoTe_2$ films by preferential sublimation of Te: Amorphous, 1T′ and 2H phases. *Journal of Materials Chemistry C*, 10 (29), 10627–10635. https://doi.org/10.1039/D2TC01281B (In English)

Huang, H. H., Fan, X., Singh, D. J. et al. (2016) Controlling phase transition for single-layer $MTe_2$ (M = Mo and W): Modulation of the potential barrier under strain. *Physical Chemistry Chemical Physics*, 18 (5), 4086–4094. https://doi.org/10.1039/C5CP06706E (In English)

Huang, J.-H., Hsu, H.-H., Wang, D. et al. (2019) Polymorphism control of layered $MoTe_2$ through two-dimensional solid-phase crystallization. *Scientific Reports*, 9, article 8810. https://doi.org/10.1038/s41598-019-45142-x (In English)

Huang, J.-H., Deng, K.-Y., Liu, P.-S. et al. (2017) Large-area 2D layered $MoTe_2$ by physical vapor deposition and solid-phase crystallization in a tellurium-free atmosphere. *Advanced Materials Interfaces*, 4 (17), article 1700157. http://dx.doi.org/10.1002/admi.201700157 (In English)

Knop, O., Haraldsen, H. (1956) A note on the system wolfram-tellurium. *Canadian Journal of Chemistry*, 34 (8), 1142–1145. https://doi.org/10.1139/v56-149

Kolobov, A. V., Tominaga, J. (2016) *Two-dimensional transition-metal dichalcogenides. Springer Series in Materials Science. Vol. 239*. Cham: Springer Publ., 538 p. https://doi.org/10.1007/978-3-319-31450-1 (In English)

Kolobov, A. V., Fons, P., Tominaga, J. (2016) Electronic excitation-induced semiconductor-to-metal transition in monolayer $MoTe_2$. *Physical Review B*, 94 (9), article 094114. https://doi.org/10.1103/PhysRevB.94.094114 (In English)

Kolobov, A. V., Lyubin, V. M., Taguyrdzhanov, M. A. (1982) Effect of pressure on photoinduced changes in chalcogenide vitreous semiconductors. *Solid State Communications*, 41 (6), 453–455. https://doi.org/10.1016/0038-1098(82)90523-3 (In English)

Krbal, M., Prokop, V., Kononov, A. A. et al. (2021) Amorphous-to-crystal transition in quasi-two-dimensional $MoS_2$: Implications for 2D electronic devices. *ACS Applied Nano Materials*, 4 (9), 8834–8844. https://doi.org/10.1021/acsanm.1c01504 (In English)

Li, N., Wang, Q., Shen, C. et al. (2020) Large-scale flexible and transparent electronics based on monolayer molybdenum disulfide field-effect transistors. *Nature Electronics*, 3, 711–717. https://doi.org/10.1038/s41928-020-00475-8 (In English)

Li, Y., Duerloo, K.-A. N., Wauson, K., Reed, E. J. (2016) Structural semiconductor-to-semimetal phase transition in two-dimensional materials induced by electrostatic gating. *Nature Communications*, 7, article 10671. https://doi.org/10.1038/ncomms10671 (In English)

Lin, Y.-F., Xu, Y., Wang, S.-T. et al. (2014) Ambipolar $MoTe_2$ transistors and their applications in logic circuits. *Advanced Materials*, 26 (20), 3263–3269. https://doi.org/10.1002/adma.201305845 (In English)

Liu, T., Liu, Z. (2018) 2D $MoS_2$ nanostructures for biomedical applications. *Advanced Healthcare Materials*, 7 (8), article 1701158. https://doi.org/10.1002/adhm.201701158 (In English)

Mak, K. F., Lee, C., Hone, J. et al. (2010) Atomically thin $MoS_2$: A new direct-gap semiconductor. *Physical Review Letters*, 105 (13), article 136805. https://doi.org/10.1103/PhysRevLett.105.136805 (In English)

Park, J. C., Yun, S. J., Kim, H. et al. (2015) Phase-engineered synthesis of centimeter-scale 1T′-and 2H-molybdenum ditelluride thin films. *ACS Nano*, 9 (6), 6548–6554. https://doi.org/10.1021/acsnano.5b02511 (In English)

Raoux, S., Jordan-Sweet, J. L., Kellock, A. J. (2008) Crystallization properties of ultrathin phase change films. *Journal of Applied Physics*, 103 (11), article 114310. https://doi.org/10.1063/1.2938076 (In English)

Saito, Y., Fons, P., Kolobov, A. V., Tominaga, J. (2015) Self-organized van der Waals epitaxy of layered chalcogenide structures. *physica status solidi (b)*, 252 (10), 2151–2158. https://doi.org/10.1002/pssb.201552335 (In English)

Saito, Y., Hatayama, S., Shuang, Y. et al. (2021) Dimensional transformation of chemical bonding during crystallization in a layered chalcogenide material. *Scientific Reports*, 11 (1), article 4782. https://doi.org/10.1038/s41598-020-80301-5 (In English)

Sarkar, D., Xie, X., Liu, W. et al. (2015) A subthermionic tunnel field-effect transistor with an atomically thin channel. *Nature*, 526 (7571), 91–95. https://doi.org/10.1038/nature15387 (In English)

Simpson, R. E., Krbal, M., Fons, P. et al. (2010) Toward the ultimate limit of phase change in $Ge_2Sb_2Te_5$. *Nano Letters*, 10 (2), 414–419. https://doi.org/10.1021/nl902777z (In English)

Song, S., Keum, D. H., Cho, S. et al. (2016) Room temperature semiconductor–metal transition of $MoTe_2$ thin films engineered by strain. *Nano Letters*, 16 (1), 188–193. https://doi.org/10.1021/acs.nanolett.5b03481 (In English)

Suzuki, R., Sakano, M., Zhang, Y. J. et al. (2014) Valley-dependent spin polarization in bulk $MoS_2$ with broken inversion symmetry. *Nature Nanotechnology*, 9 (8), 611–617. https://doi.org/10.1038/nnano.2014.148 (In English)

Tang, J., Wang, Q., Tian, J. et al. (2023) Low power flexible monolayer MoS2 integrated circuits. *Nature Communications*, 14 (1), article 3633. https://doi.org/10.1038/s41467-023-39390-9 (In English)

Thurmond, C. D., Kowalchik, M. (1960) Germanium and silicon liquidus curves. *The Bell System Technical Journal*, 39 (1), 169–204. https://doi.org/10.1002/j.1538-7305.1960.tb03927.x (In English)

Ueno, K., Fukushima, K. (2015) Changes in structure and chemical composition of α-$MoTe_2$ and β-$MoTe_2$ during heating in vacuum conditions. *Applied Physics Express*, 8 (9), article 095201. https://doi.org/10.7567/APEX.8.095201 (In English)

Wei, W., Dai, Y., Huang, B. (2017) Straintronics in two-dimensional in-plane heterostructures of transition-metal dichalcogenides. *Physical Chemistry Chemical Physics*, 19 (1), 663–672. https://doi.org/10.1039/C6CP07823K (In English)

Xiao, D., Liu, G.-B., Feng, W. et al. (2012) Coupled spin and valley physics in monolayers of $MoS_2$ and other group-VI dichalcogenides. *Physical Review Letters*, 108 (19), article 196802. https://doi.org/10.1103/PhysRevLett.108.196802 (In English)

Yin, L., Zhan, X., Xu, K. et al. (2016) Ultrahigh sensitive $MoTe_2$ phototransistors driven by carrier tunneling. *Applied Physics Letters*, 108 (4), article 043503. https://doi.org/10.1063/1.4941001 (In English)

Yoo, Y., DeGregorio, Z. P., Su, Y. et al. (2017) In-plane 2H-1T′ $MoTe_2$ homojunctions synthesized by flux-controlled phase engineering. *Advanced Materials*, 29 (16), article 1605461. https://doi.org/10.1002/adma.201605461 (In English)

Zachariasen, W. H. (1932) The atomic arrangement in glass. *Journal of the American Chemical Society*, 54 (10), 3841–3851. https://doi.org/10.1021/ja01349a006 (In English)

Zhao, C., Batiz, H., Yasar, B. et al. (2021) Tellurium single-crystal arrays by low-temperature evaporation and crystallization. *Advanced Materials*, 33 (37), article 2100860. https://doi.org/10.1002/adma.202100860 (In English)

Zhou, L., Xu, K., Zubair, A. et al. (2015) Large-area synthesis of high-quality uniform few-layer $MoTe_2$. *Journal of the American Chemical Society*, 137 (37), 11892–11895. https://doi.org/10.1021/jacs.5b07452 (In English)

Zhou, L., Zubair, A., Wang, Z. et al. (2016) Synthesis of high-quality large-area homogenous 1T′ $MoTe_2$ from chemical vapor deposition. *Advanced Materials*, 28 (43), 9526–9531. https://doi.org/10.1002/adma.201602687 (In English)